Int. J. Multiphase Flow Vol. 11, No. 6, pp. 761–782, 1985
Printed in Great Britain.

0301-9322/85 $3.00 + .00

TWO-PHASE FLOW PATTERNS AND VOID FRACTIONS IN DOWNWARD FLOW
PART I: STEADY-STATE FLOW PATTERNS

T. J. CRAWFORD†, C. B. WEINBERGER
Drexel University, Philadelphia, Pennsylvania, U.S.A.

and

J. WEISMAN
University of Cincinnati, Cincinnati, Ohio, U.S.A.

(*Received* 6 *September* 1984; *in revised form* 5 *February* 1985)

Abstract—Observations of void fractions and flow patterns have been made during steady-state, co-current, downward flow of liquid refrigerant 113 and its vapor. The new data on flow pattern transitions, plus the available downward flow data in the literature, have been compared with available predictions. It was found that the flow pattern map previously developed for horizontal and upward flow can be extended to downward flow with only minor modifications. Part II of this paper will report on the void fraction measurements and the observations of flow pattern transitions during flow transients.

1. INTRODUCTION

Most studies of two-phase, co-current gas–liquid flow have been conducted in either horizontal lines or with upward flow in vertical lines. Relatively little work has been directed toward flow in vertically downward lines or lines declined at various angles.

The experimental flow pattern studies carried out in vertically downward flow are those of Oshinowo & Charles (1974), Golan & Stenning (1969), Yamazaki & Yamaguchi (1979), Spedding & Nguyen (1980) and Barnea *et al.* (1982). Nearly all of these investigators used air and water in line sizes of about 2.5 cm. (Barnea *et al.* also examined a 5-cm line). Oshinowo & Charles (1974) also looked at the air–glycerine–water system. Despite the fact that nearly all of these investigators have studied the air–water at near atmospheric pressure and the same size lines, there is substantial scatter in the observed flow pattern transitions.

Flow patterns in lines declined at various angles other than the vertical have only been observed by Spedding & Nguyen (1980) and Barnea *et al.* (1982). Again only the air–water system was examined.

No general agreement on the appropriate procedure for presenting flow pattern maps in downward flow has been reached. Oshinowo & Charles (1974) plotted the square root of the ratio of gas and liquid volumetric flow rates versus a two-phase Froude number adjusted for fluid properties. Somewhat similar coordinates were used by Spedding & Nguyen (1980) by Yamazaki & Yamaguchi (1979), Golan & Stenning (1969) and Barnea *et al.* (1982) simply plotted superficial gas velocity versus superficial liquid velocity. Barnea *et al.* (1982) also developed phenomenological models which used several dimensionless groups.

In view of the scatter in the available data as well as the absence of any data with high density vapor, it was decided to conduct a series of flow pattern visualization experients using liquid refrigerant 113 and its vapor. Further, since void fraction data was also limited in downward flow, it was decided to obtain data on the relationship between quality and void fraction at the same time.

Part I of this paper presents the flow pattern studies carried out during steady state. Part

†Current address: American Electric Power, Columbus, Ohio

II will present the void fraction data and the observations of flow patterns during flow transients.

2. EXPERIMENTAL PROGRAM

The experimental data were obtained with the University of Cincinnati's boiling refrigerant loop using refrigerant 113 (molecular wt. = 187.4) as the working fluid. The loop is illustrated in figure 1.

The facility is capable of pumping up to 1.8 m^3/s of refrigerant 113 through electric heaters which produce a two-phase mixture. The two-phase mixture then flows downward through a 1.5 m long glass tube in which the flow pattern is observed visually. Glass tubes with internal diameters of 2.5 cm and 3.8 cm were used for the test section. Since only configurations were observed, no parallax correcting devices were needed.

In all cases the test section was preceded by a section of pipe having a diameter very close to that of the test section and a length of about 1.3 m. The total L/D ratio for the constant diameter line was therefore approximately 110 for the small line and 75 the large line. Previous studies (Weisman *et al.* 1979) had shown that, even when the gas and liquid were first mixed at the entrance of the test section, no significant entrance effects on flow patterns were observed at such values of L/D. Under conditions where the vapor and liquid were flowing together prior to entering the test line, even less of an L/D effect may be expected. The absence of significant L/D effects in the present case was confirmed by the fact that there was essentially no difference in flow pattern observations taken at the middle and end of the glass test section.

The two-phase mixture leaving the test section flows through a short section of steel pipe (same diameter as test section) and then a flexible line which allows for expansion. The fluid then enters a condensor, the single phase liquid leaving the condensor is recirculated. The system is maintained at the desired pressure by a bladder-type accumulator connected to the pump discharge line. The system was operated at pressures of 2 and 4 bars absolute.

The total liquid flow was measured by an orifice meter and the two-phase mixture flow was measured with a drag disk preceded by a fine screen. Previous studies (Weisman 1977)

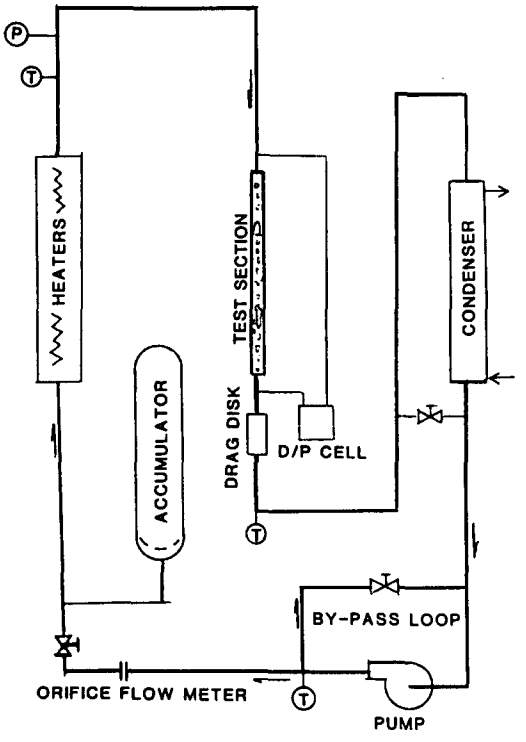

Figure 1. Boiling freon loop.

have shown that the drag disk signal was proportional to $(G_T^2/\bar{\rho})$ where $\bar{\rho}$ is the homogeneous mixture density and G_T is the total mass flow. As G_T is known from the liquid flow measurement, the value of ρ for a homogeneous mixture is obtained from the drag disk reading. The quality is the then readily obtained from $\bar{\rho}$.

Void fractions were obtained by measuring the differential pressure across the test section with a bellows-type differential pressure cell. After appropriately correcting for pipe friction, the elevation head could be obtained. The density derived from the elevation head provided the desired void fraction data. Since the contribution of friction to the total elevation head was small, generally less than 8% of the total pressure drop, the procedure was capable of providing good accuracy.

Experimental data were obtained with the 2.5 cm tube at downward angles of 90°, 60°, 45°, 30° and 15°. The 3.8 cm diameter tube was used only at 90°. All configurations were tested at both 2 bar and 4 bar absolute. Because the differential elevation head was too low to provide accurate density values at the 30° and 15° angles, no direct determination of void fractions was made at these angles. Additional details are available from Crawford (1983).

3. EXPERIMENTAL FLOW PATTERNS OBSERVATIONS

The visually observed flow patterns were categorized in a manner generally consistent with that used by Weisman & Kang (1981) in their classification of co-current upward flow. They indicated that the flow observations could be divided into bubble, annular, intermittent, separated and dispersed regions. In downward flow, these same general categories may be retained with only minor modifications.

Bubble flow means small discrete bubbles of various diameters (all significantly less than the tube diameter) moving in the direction of the liquid but generally not at the liquid velocity. In vertically downward flow, the bubbles tended to be ellipsoidal or spherical at the high flow rates but hemispherical (umbrealla shaped) at the lower flow rates (see figure 2). In vertical lines, the smaller, faster-moving bubbles tended to move towards the center of the

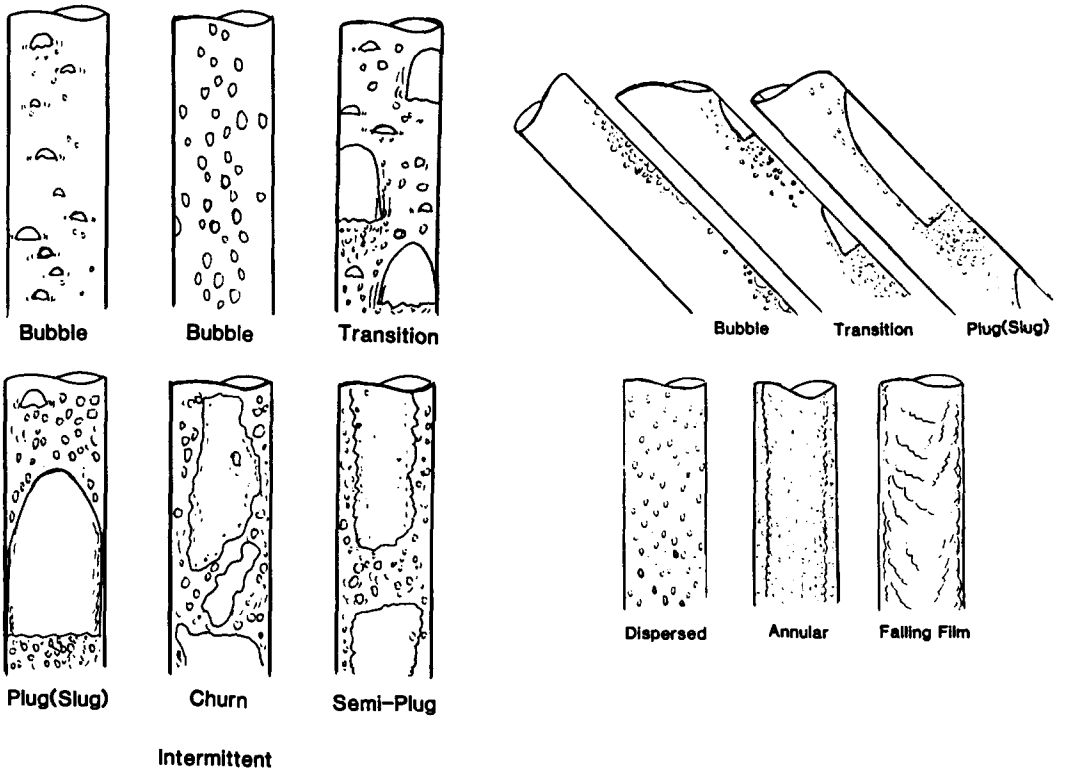

Figure 2. Flow pattern configurations seen in downward flow.

pipe while the larger slower-moving ones were found near the wall. In lines declined at other angles, the bubbles rose to the top of the tube and tended to coalesce more readily.

Intermittent flow is used to describe the flow pattern in which there are alternating vapor and liquid packets. Included within this region is plug flow (sometimes called slug flow) where large Taylor plugs of gas are found. These gas bubbles with hemispherical caps nearly filled the entire tube and moved upward with respect to the liquid, but the drag and viscous forces were always sufficient to give them a net downward velocity. This plug flow was only seen near the bubble–intermittent transition. As one moved away from the transition the gas plugs did not fill the entire tube and did not have a hemispherical head (see figure 2). This region was designated as "semiplug."

The intermittent region also includes "churn" flow where there is a chaotic mixture of vapors and liquid packets (see figure 2). This behavior was observed only in the vertical lines and was more prominent at the higher pressure.

In upward flow in inclined or vertical lines, annular flow is characterized by the presence of a continuous liquid film around the outer surface of the tube and a central gas core which generally contains liquid droplets. The same definition may be used with flow in lines declined to the vertical. This will distinguish the flow pattern from separated flow where there is a liquid layer only along the bottom portion of the tube.

The foregoing distinction between annular and separated flow is not readily applicable in vertically downward flow. Under these conditions, a "falling film" flow, which is characterized by liquid layers that trickle down the walls will be encountered. The liquid layers appear to flow gently over one another as sheets. The vapor flows in the center core. In vertical lines,

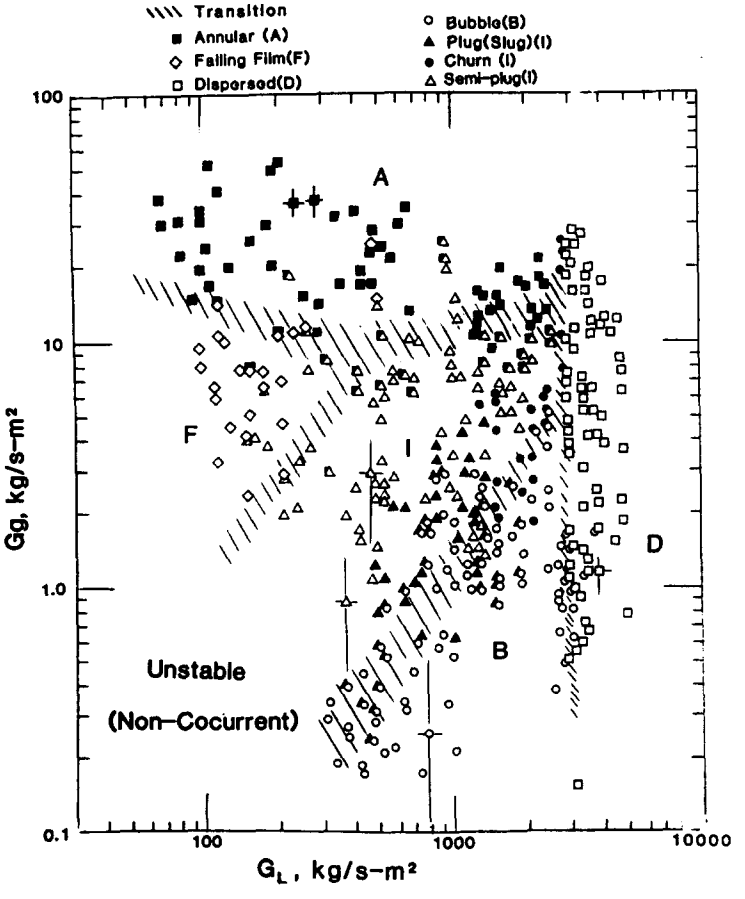

Figure 3. Flow pattern map: $D = 2.5$ cm $\theta = -90°$ $P = 2$ bar refrig. 113

annual flow was distinguished from falling film by the relatively large amount of droplet entrainment in the vapor core, the high-speed driving motion of the mixture being blown through the tubes and the absence of layers flowing over each other in sheets. Generally numerous tiny (dia $\leq$ 1 mm) bubbles appeared to be dispersed in the liquid layer on the wall during annular flow.

Flow pattern maps were prepared using the flow pattern categorization indicated in the foregoing paragraphs. The basic maps, shown in figures 3–8, were drawn in terms of the superficial gas and liquid mass fluxes. Each observation is represented by a symbol indicating the observed flow pattern, at the appropriate G_G, G_L coordinates. The shaded regions represent the boundaries between the various flow pattern regions. In drawing these boundaries, the "plug," "semi-plug" and "churn" flows were all treated as part of the "intermittent" flow pattern. No attempt was made to define the boundaries of the subregions of intermittent flow. In a few cases it was difficult to assign the flow pattern to a subregion and then the simple "intermittent" designation was used.

Figures 3 and 4 show the flow maps obtained for vertically downward flow in the 2.5 cm tube at ~2 bar and ~4 bar absolute. The maps are similar in many respects to those obtained in upward or horizontal flow. As in upward flow, dispersed flow is seen only at high mass velocities and the transition occurs at a nearly constant liquid mass velocity, $G_L \simeq 3000$ kg/m^2 S. The general positions of intermittent and bubbly flow are similar to those seen in upward flow. Falling film flow takes in the general region in which stratified flow is seen in horizontal lines.

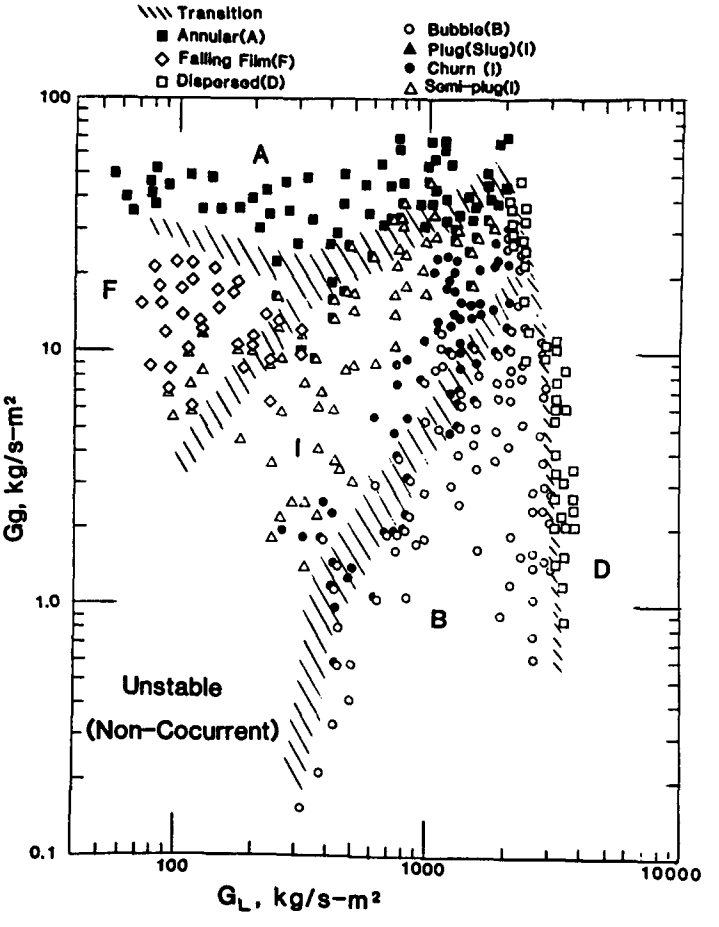

Figure 4. Flow pattern map: D = 2.5 cm θ = −90° P = 4 bar refrig. 113

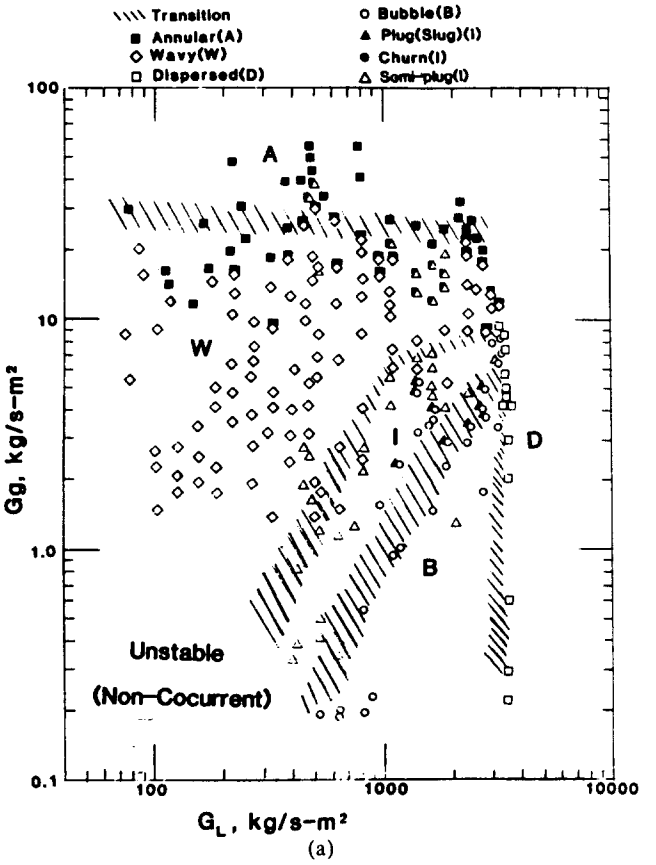

(a)

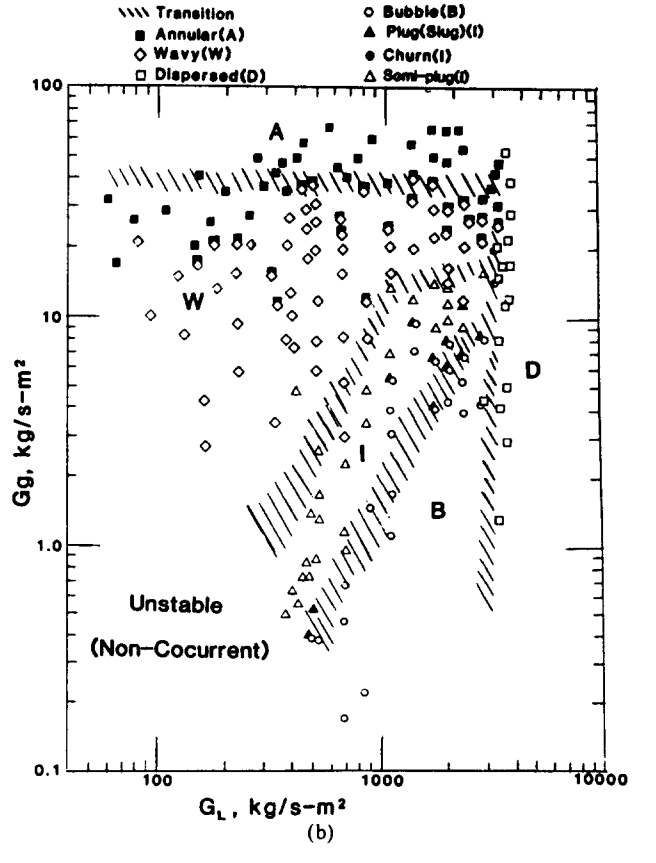

(b)

Figure 5. Flow pattern maps for $\theta = -15°$ (refrig. 113). (a) $P = 2$ bar; (b) $P = 4$ bar.

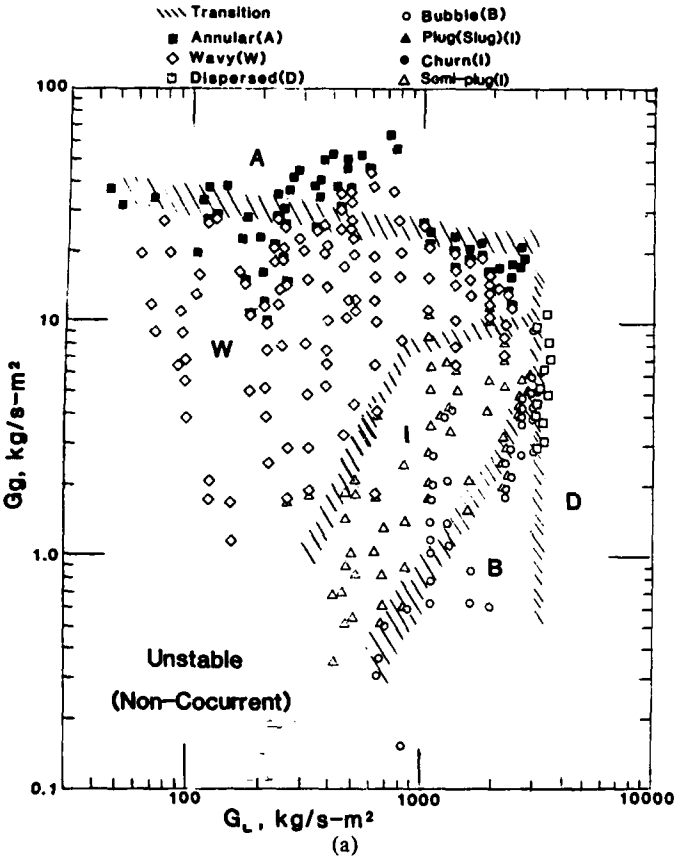

(a)

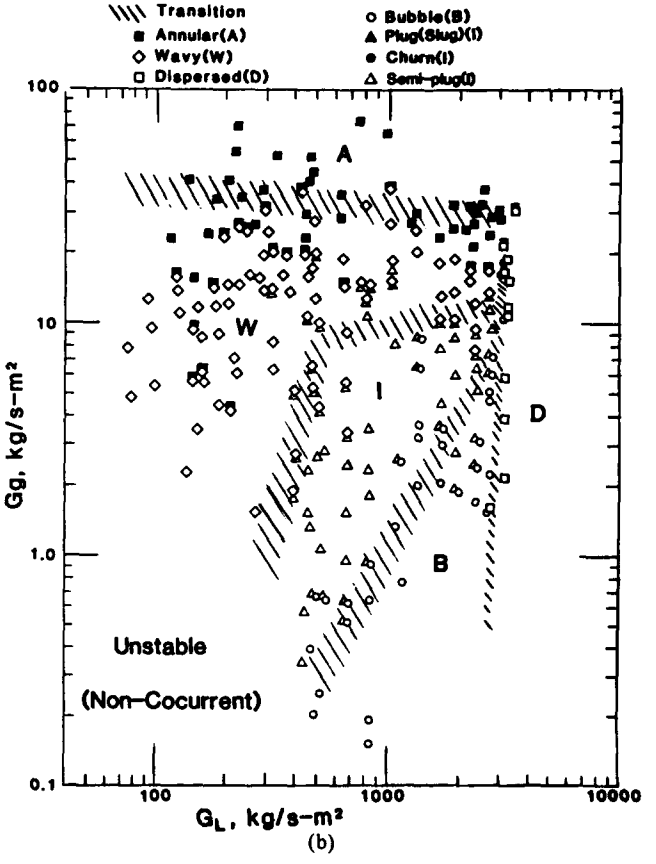

(b)

Figure 6. Flow pattern maps for $\theta = -30°$ (refrig. 113). (a) $P = 2$ bar; (b) $P = 4$ bar.

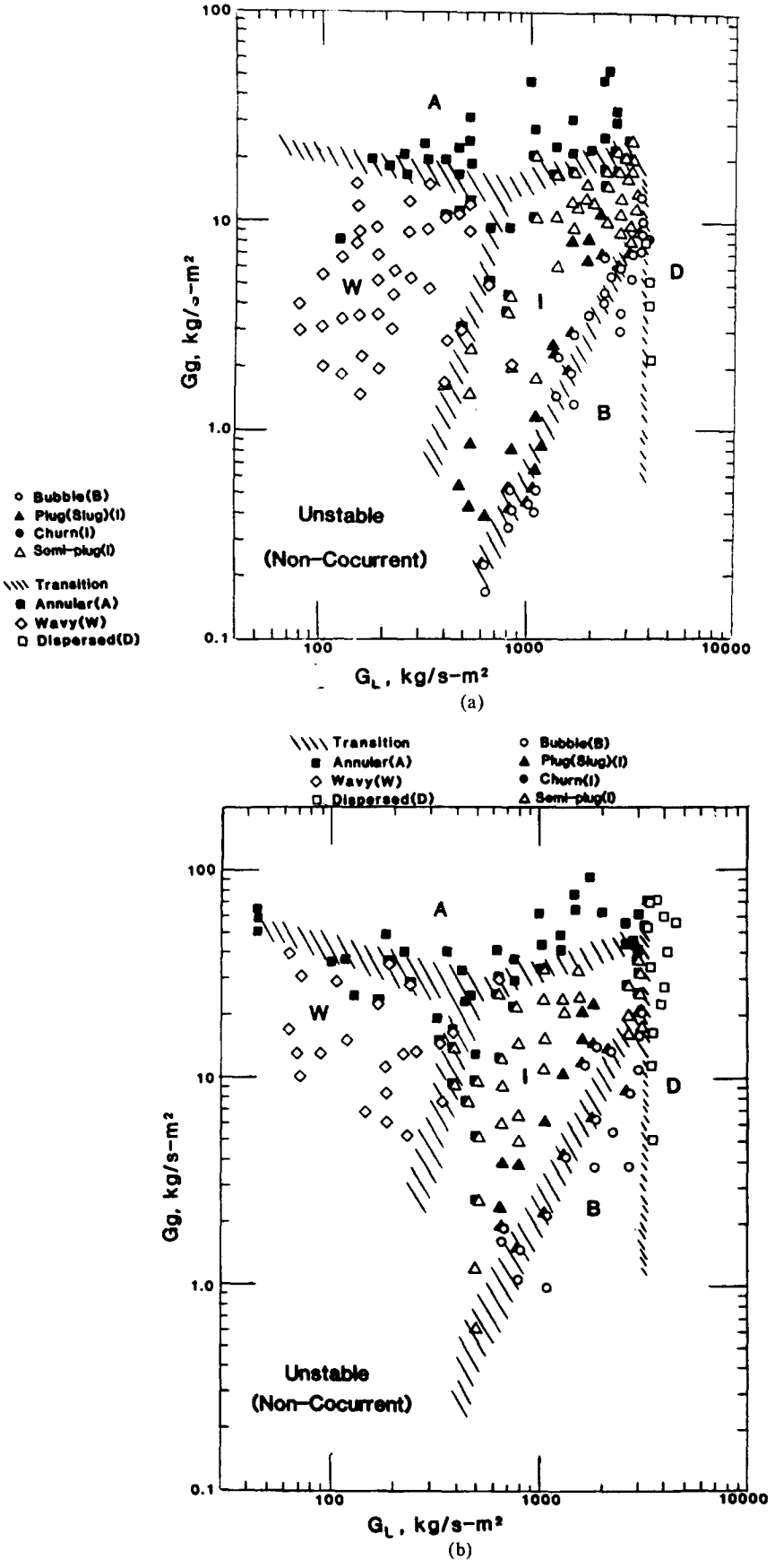

Figure 7. Flow pattern maps for $\theta = -45°$ (refrig. 113). (a) $P = 2$ bar; (b) $P = 4$ bar.

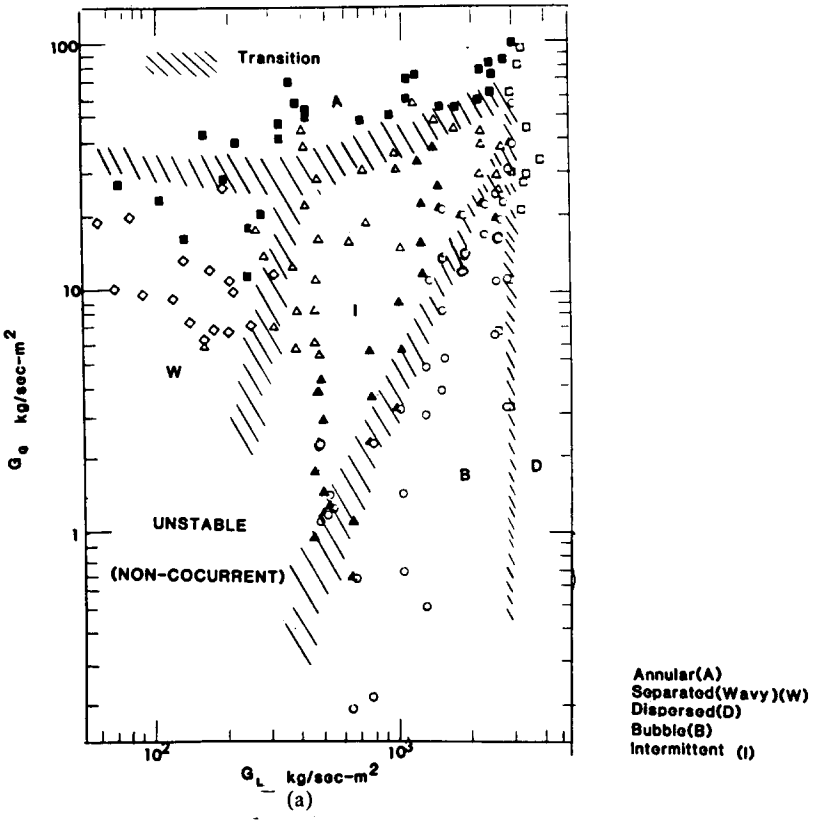

(a)

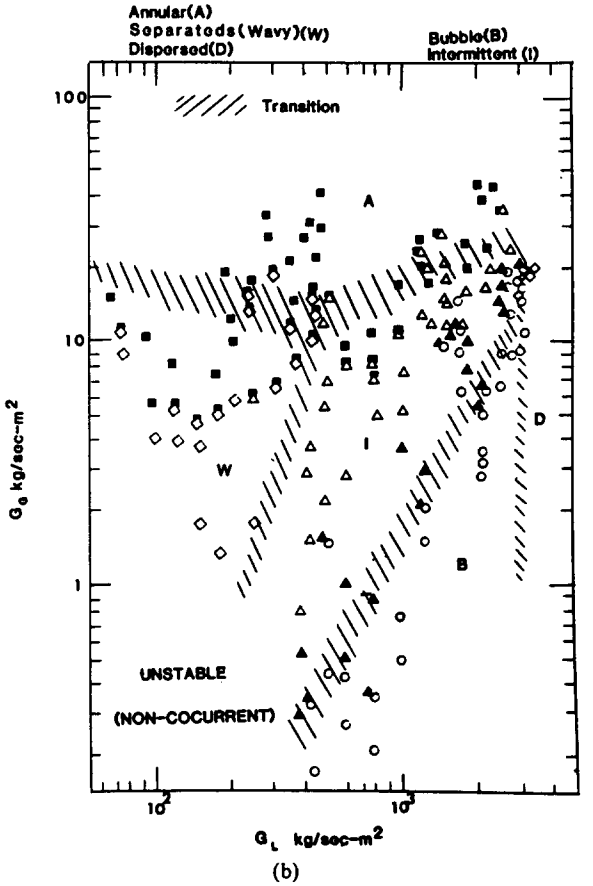

(b)

Figure 8. Flow pattern maps for $\theta = -60°$ (refrig. 113). (a) $P = 4$ bar; (b) $P = 2$ bar.

Annular flow occurs at a high gas rate which varies only slightly with liquid rate. Note, however, that because of increased gas density the mass flux at which annual flow begins at ~4 bar is about double that at which it begins at ~2 bar.

It should be noted that there was a region of low liquid and gas flows where flow pattern observations could not be made. In this region, stable system operation could not be maintained because gas could not be made to flow downwards in a continuous fashion.

Figures 5–8 show the flow pattern observations obtained at the downward angles (from horizontal) of 15°, 30°, 45° and 60° in the 2.5 cm tube. Again, tests were conducted at both ~2 bar and ~4 bar. Behavior at the sharp angles of 60° and 45° was similar to that seen in vertically downward flow. However, at the less steeply declined angles of 30° and 15° angles, the intermittent transition line has moved appreciably from the vertical and there is now a separated region between intermittent and annual flow.

The significant expansion of the separated region in lines declined at 15° and 30° is consistent with the observation of Gibson (1981). Gibson examined the air–water system in both 2.5 and 5.1 cm lines which were declined at a 7° angle. He observed a noticeable increase (relative to horizontal flow) of the separated region at the expense of the intermittent region (see figure 9). The transitions to annular and dispersed flow were essentially the same as for horizontal flow.

An alternative way of mapping flow patterns is to use the coordinates of void fraction, α, and total mass flux, G_T. This has been done in figures 10a and 10b where the behavior at 2 bar in vertically downward flow and flow in a line declined at 60° is shown. With these coordinates, the region for separated flow is very small at the for these steep declination angles. However, consistent with the G_G vs G_L maps, there would be an appreciable separated region in an α vs G_T map at a low angle of declination.

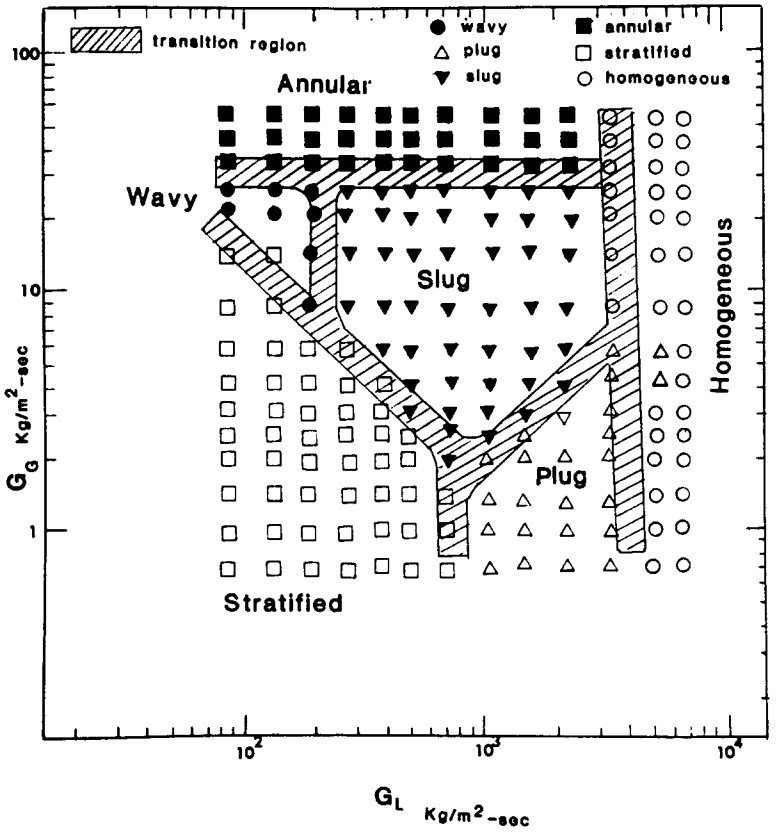

Figure 9. Flow pattern map for $\theta = 7°$ (air-water system)

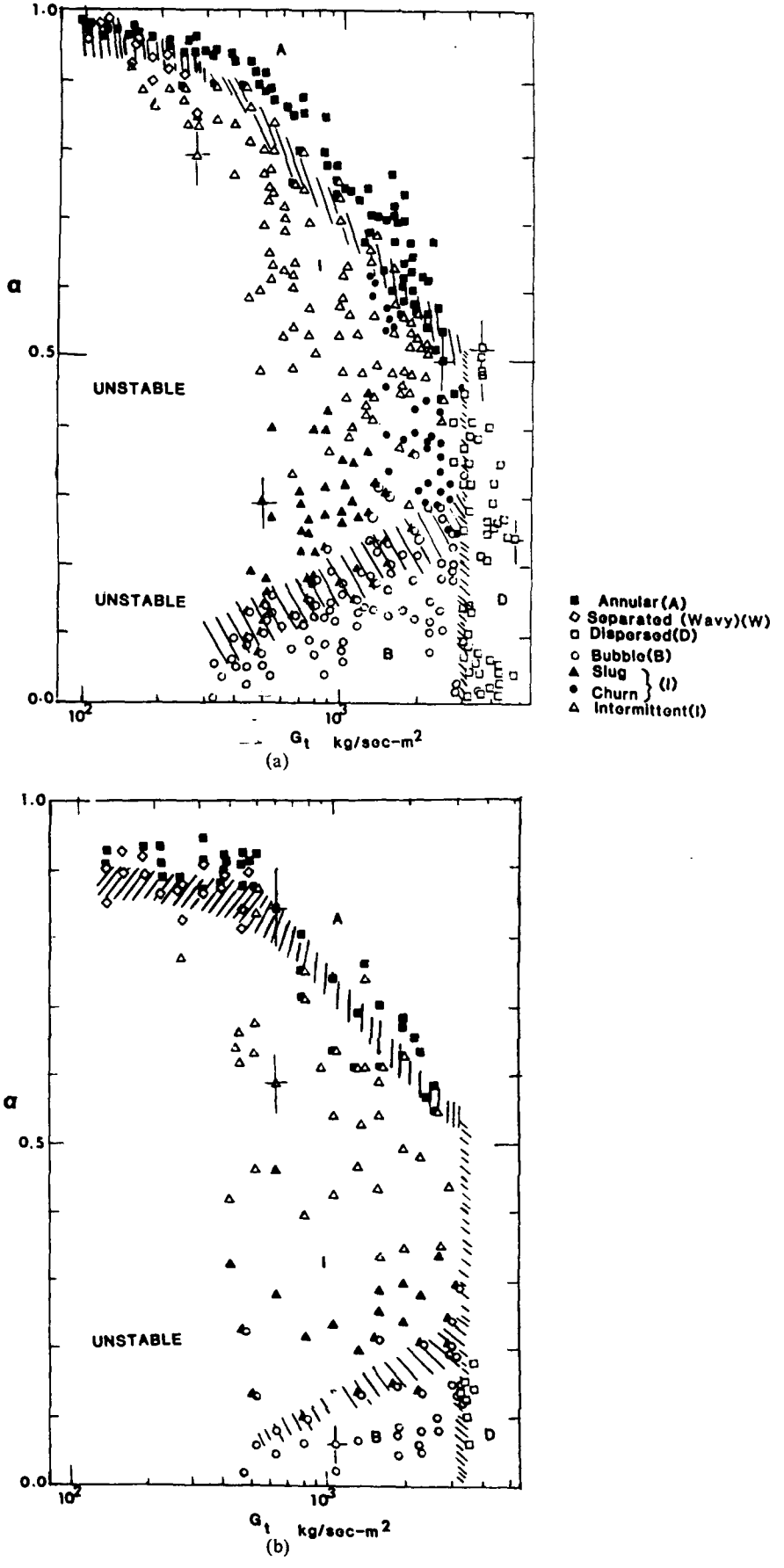

Figure 10. Flow pattern maps in terms of void fraction and total mass flow rate (D = 2.5cm). (a) P = 2 bar, $\theta = -90°$; (b) P = 2 bar, $\theta = -60°$.

4. COMPARISON WITH AVAILABLE FLOW PATTERN TRANSITION PREDICTIONS

A number of approaches have been taken to the prediction of flow pattern transitions. One of the useful approaches has been that due to Weisman et al. (1979) and Weisman & Kang (1981). They recognized that the appropriate dimensionless correlating groups depended on the particular transition and obtained separate correlations for each significant transition as shown below.

Transition to annual flow

$$1.9(V_{SG}/V_{SL})^{1/8} = Ku_G^{0.2} Fr_G^{0.18}. \quad [1]$$

Separated–intermittent transition

$$(Fr_G)^{1/2} = 0.25(V_{SG}/V_{SL})^{1.1}. \quad [2]$$

Transition to dispersed flow

$$\left[\frac{|\, dp/\mathrm{dx}\,|_{SL}}{(\rho_L - \rho_G)g}\right]^{1/2}\left[\frac{\sigma}{(\rho_L - \rho_G)gD^2}\right]^{1/4} = 1.7.‡ \quad [3]$$

Bubble to intermittent transition

$$\frac{V_{SG}}{\sqrt{gD}} = 0.45\left(\frac{V_{SG} + V_{SL}}{\sqrt{gD}}\right)^{0.78}(1 - 0.65\cos\theta), \quad [4]$$

where $|\, dp/dx\,|^{SL}$ = absolute value of pressure drop for liquid flowing alone per unit length
D = pipe diameter (L)
$Fr_G = V_{SG}^2/(gD)$,
g = acceleration due to gravity (M/TL^2)
$Ku_G = V_{SG}(\rho_G)^{1/2}/[g(\rho_L - \rho_G)\sigma]^{1/4}$
$V_{SG}V_{SL}$ = superficial gas and liquid velocities, respectively, based on one phase flowing alone (L/G)
ρ_G, ρ_L = gas and liquid densities, respectively (M/L^3)
σ = interfacial tension (F/L)
θ = angle of inclination

These correlations apply to both horizontal and upward flow (vertical or inclined) with the exception that the separated–intermittent transition is not seen in vertically upward flow. Recently, Crawford & Weisman (1984) showed that these transition line predictions, which were obtained for adiabatic flow provided reasonable predictions of available diabatic flow data. In addition, they give reasonable predictions of the available data on adiabatic flow in annuli and rod bundles. However, Crawford & Weisman (1984) suggested that, at values of $(V_{SG} + V_{SL}/\sqrt{gD})$ above 1.3, the bubble–intermittent prediction is improved by using

$$\frac{V_{SG}}{\sqrt{gD}} = 0.35\left[\frac{V_{SG} + V_{SL}}{\sqrt{gD}}\right]^{1.1}(1 - 0.65\cos\theta) \quad [5]$$

instead of [4].

The transition line correlations were reduced to a simple flow map with coordinates of V_{SG}/ϕ_1 and V_{SL}/ϕ_2. By defining ϕ_1 and ϕ_2 differently for each transition, the differing effects of fluid properties and line size could be handled. The flow map of Weisman *et al.* (1979)

‡Due to a typographical error, the constant 1.7 was given incorrectly as 9.7 in previous work.

and Weisman & Kang (1981) is indicated in figure 11. The map shown has been slightly modified as suggested by Weisman (1984). Weisman used the data of Pearce (1982) to establish the behavior of the dispersed flow transition at high qualities.

The proposed flow map has also been compared with the recent studies of the intermittent annular flow transition by Iwasyk & Green (1982). These studies with very viscous liquids (2 to 17 poise) agreed very well with flow map predictions. Iwasyk & Green (1982) concluded that the Weisman *et al.* (1979) proposal that the annular–intermittent transition was a function only if the Kutadelaze number and Froude number was strongly supported.

The new data of Crowley *et al.* (1984) on the separated-intermittent transition have also been examined. These data were obtained in a 17 cm line with (air–water), (refrigerant 12 vapor–water) and (refrigerant 12 vapor–400 cp glycerine solution) systems. All of these systems were in generally good agreement with the Weisman *et al.* (1979) flow map. Note that the flow map prediction of the lack of a viscosity effect appears to be confirmed by these data.

4.1 *Dispersed flow*

From figures 3 through 9, one can observe that the transition to dispersed flow depends primarily on liquid mass flux, with essentially no dependence on angle of declination. Further, these transitions appear close to those seen in the earlier studies with horizontal and

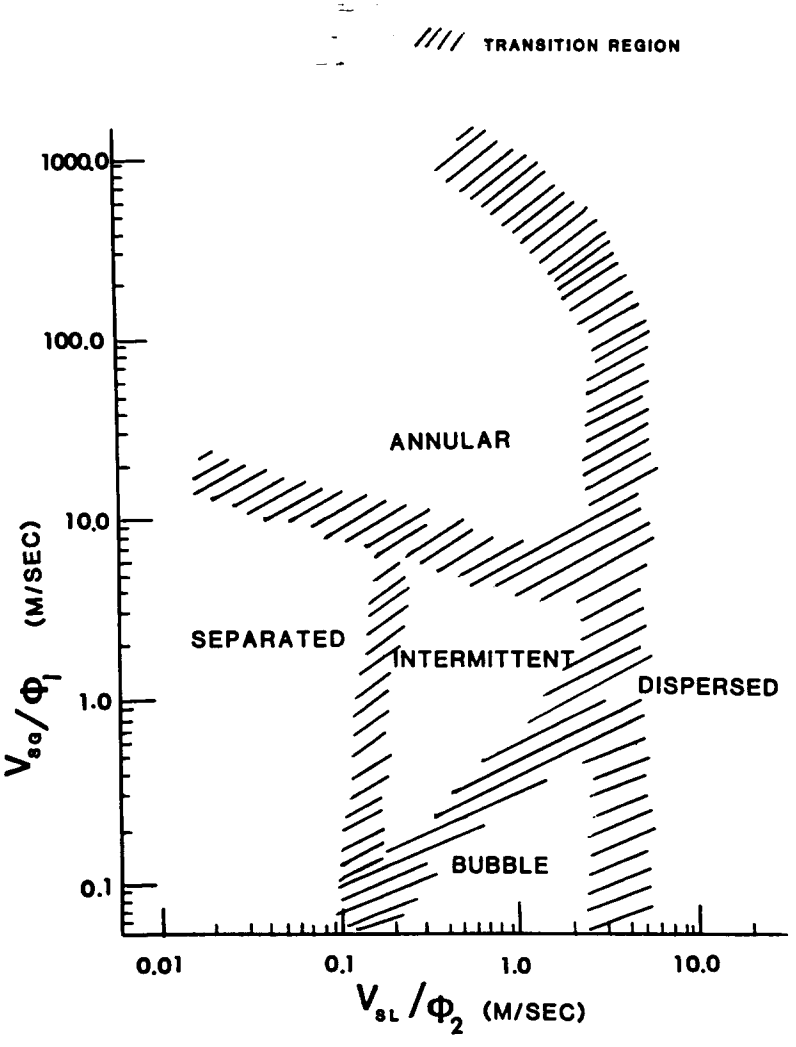

Figure 11. Generalized map for flow pattern prediction.

upward flow. Accordingly, the data of the present study were compared to the dispersed transition region suggested by Weisman & Kang (1981) in their overall flow map. This comparison is shown in figure 12 where it may be seen that the present data are in very good agreement with the prediction.

Also shown in figure 12 are (a) the downward flow data of Barnea *et al.* (1982) obtained with air–water at a variety of angles and (b) the downward flow data of Gibson (1981) obtained with air–water at a 7° angle. Good agreement is obtained with the Gibson (1981) data and reasonably good agreement with most of Barnea *et al.* (1982) data. One would therefore conclude that the Weisman & Kang (1981) flow map provides a reasonable prediction for the dispersed flow transition in downward flow.

4.2 *Annular flow*

The positions of the lines indicating the transition to annular flow appear to differ only slightly from those seen in vertical and horizontal flow. However, when the air–water data of other investigators are considered, large scatter is seen. This is in part due to the differing qualitative criteria which have been used to define the onset of annular flow.

In particular, the criteria used by Golan & Stenning (1969) and Yamazaki & Yamaguchi (1979) seemed to be substantially different than those used by other investigators. These data were therefore excluded from further consideration.

The transition lines indicating the onset of annular flow obtained in the present study are plotted on the overall flow pattern map (V_{SG}/ϕ_1 vs V_{SL}/ϕ_2) of Weisman & Kang (1981) in figure 13. Also shown are the downward air–water data of Barnea *et al.* (1982), Oshinowo & Charles (1974), Gibson (1981), and Spedding & Nguyen (1980). The shaded area represents the transition region predicted by Weisman & Kang (1981). It may be seen that the Weisman & Kang prediction provides a reasonable representation of overall behavior. It

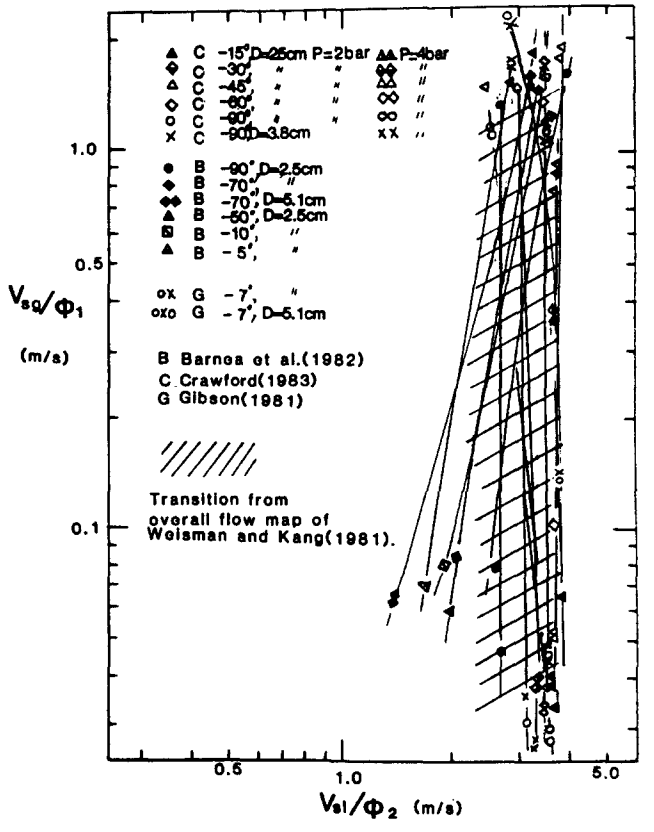

Figure 12. Comparison of predictions and observations of dispersed flow transition.

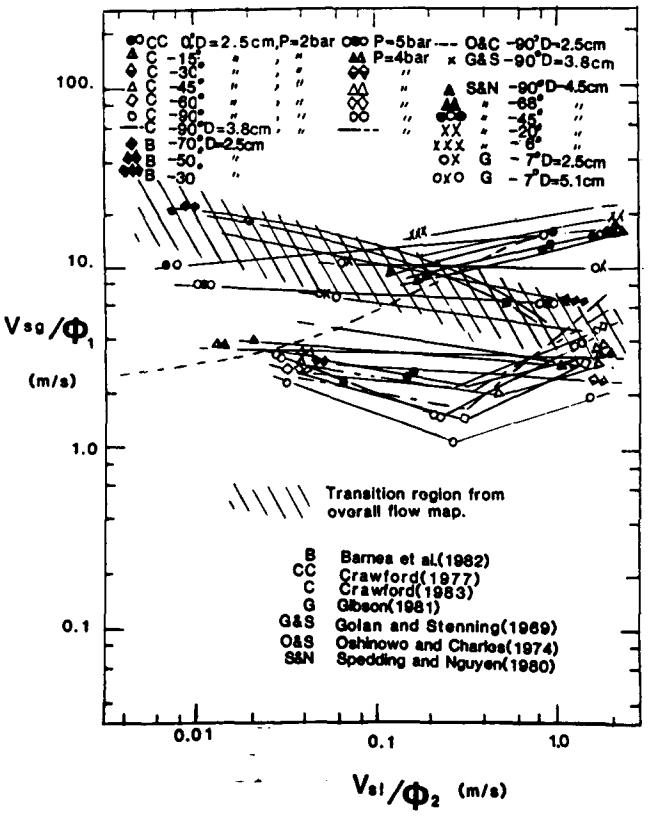

Figure 13. Comparison of predictions and observations of annular flow transition.

is a good representation of the recent air–water data of Barnea *et al.* (1982) and Gibson (1981). The freon data of the present study fall slightly below the predictions whereas the Spedding & Nguyen (1980) air–water data lie somewhat above the predictions and have a different slope. In view of the scatter of the data obtained with the same fluids and line sizes, it is believed that the Weisman & Kang predictions may be considered to be in reasonably good agreement with the downflow observations.

4.3 *Bubble–intermittent transition*

In addition to the data of the present study, the data of Golan & Stenning (1969) and Oshinowo & Charles (1974) were available. All of these observed transition lines were compared with eqns [4] and [5]. While the comparison was reasonable, an appreciably better fit could be obtained by using a revised angle correction factor and revised exponent for the mixture Froude number. The revised correlation is

$$\frac{V_{SG}}{\sqrt{gD}} = 0.18\left[\frac{V_{SG} + V_{SL}}{\sqrt{gD}}\right]^{1.6}[0.65 - 0.3(\cos\theta)^{0.3}]. \qquad [6]$$

This equation is compared to the available data in figure 14 and is observed that the prediction equation is highly successful.

4.4 *Separated–intermittent transition*

It was previously noted that, in contrast to upward flow, this transition depended on the angle with the horizontal. Hence, when the dimensionless groups of [2] were used to correlate the data, there was clearly a relationship but an additional angular dependent term was needed to reduce the spread of the data. An empirical correction was added to allow the transition to (a) move toward larger values of V_{SL} as the line change from the vertical to less

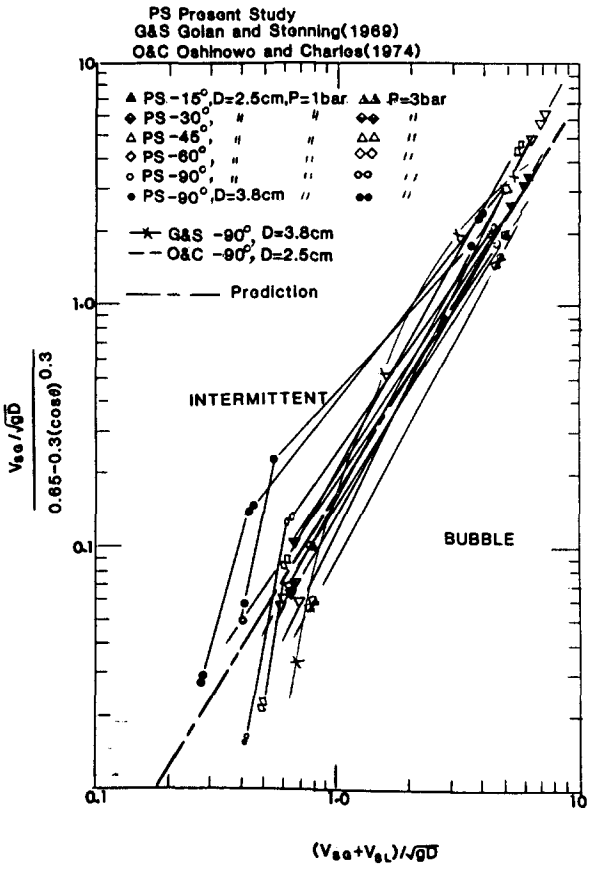

Figure 14. Comparison of predictions and observations of bubble–intermittent transition.

steep slopes and (b) shift back to lower values of V_{SL} as the angle approached the horizontal. The final equation is

$$\frac{V_{SG}}{\phi_1 \sqrt{gD}} = 0.32\left[\frac{V_{SG}}{V_{SL}}\right]^{1.1} \qquad [7]$$

where

$$\phi_1 = 1 + 4\,(\sin 1.95\|\theta\|)\exp\left[\frac{12}{3 + |\theta|}\right]$$

and θ is in degrees.

The available experimental data [present study and air–water data of Barnea *et al.* (1982), Spedding & Nguyen (1980), Gibson (1981), Golan & Stenning (1969), Oshinowo & Charles (1974)] are compared to [7] in figure 15. It will be observed that the refrigerant 113 and air–water data are brought together. Considering the scatter in the air–water data taken under similar conditions, the agreement is considered quite good.

5. OVERALL-FLOW PATTERN MAP FOR DOWNWARD FLOW

The simple-to-use, overall flow pattern map (see figure 11) proposed by Weisman *et al.* (1979) may be adapted to downward flow by defining appropriate values for ϕ_1 and ϕ_2. The annual and dispersed transition lines remain unchanged in downflow and hence ϕ_1 and ϕ_2 are

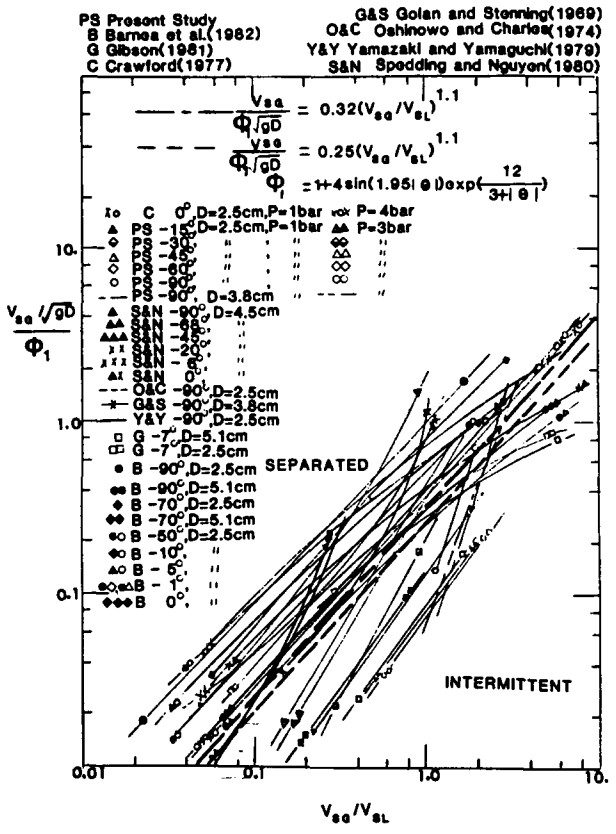

Figure 15. Comparison of predictions of observations of separated–intermittent transition.

unchanged. The separated–intermittent line must be revised in accordance with [7] and the bubble–intermittent line revised in accordance with [6]. The revised values of ϕ_1 and ϕ_2 needed are given in table 1. The table also reflects the revisions of Weisman (1984).

It should be noted that there are slight discrepancies between the estimates of the separated–intermittent transition obtained with the near-horizontal and downward lines as the inclination angle approaches zero. Although both equations describing the separated intermittent transition [2] and [7] have the same form and $\phi_1 = 1.0$ in both equations when $\theta = 0$, the constant coefficients in front of these equations are somewhat different and hence ϕ_2 is not identical. A discrepancy is also seen in the equations describing the bubble–intermittent transition. Again, the angle correction factor for downflow reduces to that for horizontal flow when $\theta = 0$ but the exponent on the total Fourde number is higher for downward flow. This is partly compensated for by a lower constant multiplying the right-hand side. At small declination angles it is probably desirable to estimate this transition location by averaging the results of the downflow and horizontal relationships.

6. COMPARISON OF DATA WITH PREDICTIONS OF BARNEA *et al.* (1982)

The theoretically based predictions of Barnea *et al.* (1982) have also been compared to the data obtained in the present study. Barnea did not identify a bubble region and hence the bubble–intermittent transition could not be compared. The data of the present study obtained for the separated–intermittent transition at ~4 bar are compared to the Barnea *et al.* predictions in figure 16. As may be seen, only very rough agreement between experiment and theory is seen. Similar behavior is observed for the data at ~2 bar. Most notable is the difference in the flow angle dependence of the predictions and the data. The data moves toward increased values of V_{SL} as the angle becomes less steep but the predictions move to lower values of V_{SL}.

Table 1. Property and Pipe Diameter Corrections to Overall Flow Map*

Transition	Flow Orientation	ϕ_1	ϕ_2
To Dispersed Flow	All	$\left(\frac{\rho_{GS}}{\rho_G}\right)\left(\frac{\rho_L}{\rho_{LS}}\right)^{0.67}\left(\frac{D}{D_S}\right)^{0.21}\left(\frac{\mu_{LS}}{\mu}\right)^{0.09}\left(\frac{\sigma}{\sigma_S}\right)^{0.24}$	$\left(\frac{\rho_L}{\rho_{LS}}\right)^{0.33}\left(\frac{D}{D_S}\right)^{0.21}\left(\frac{\mu_{LS}}{\mu_L}\right)^{0.09}\left(\frac{\sigma}{\sigma_S}\right)^{0.24}$
To Annular Flow	All	$\left(\frac{\rho_{GS}}{\rho_G}\right)^{0.23}\left(\frac{\Delta\rho}{\Delta\rho_S}\right)^{0.11}\left(\frac{\sigma}{\sigma_S}\right)^{0.11}\left(\frac{D}{D_S}\right)^{0.415}$	1.0
Intermittent-Separated	a) Horizontal and Slightly inclined	1.0	$\left(\frac{D}{D_S}\right)^{0.45}$
	b) Sharply inclined c) Downward	separated flow disappears $\left[1 + 4\,(\sin 1.95\,\lvert\theta\rvert)\exp\left(\frac{12}{3 + \lvert\theta\rvert}\right)\right]$	$1.25\left(\frac{D}{D_S}\right)^{0.45}$
Bubble-Intermittent	a) Horizontal and upward	$\left(\frac{D}{D_S}\right)^{0.8}(1 - 0.65\cos\theta)$	$\frac{D}{D_S}$
	b) Downward	$\left(\frac{D_S}{D}\right)^{0.19}[0.65\text{–}0.3\,(\cos\theta)^{0.3}]\left[0.6\left(\frac{V_{SL}}{V_{SG}}\right)^{0.73}\right]$	1.0

*S denotes standard conditions. D_S = 1.0 in. = 2.54 cm, ρ_{GS} = 0.0013 kg/l, ρ_{LS} = 1.0 kg/l. μ_{LS} = 1 cP. σ_S = .07 N/m (70 dynes/cm) $\Delta\rho = \rho_L - \rho_G$

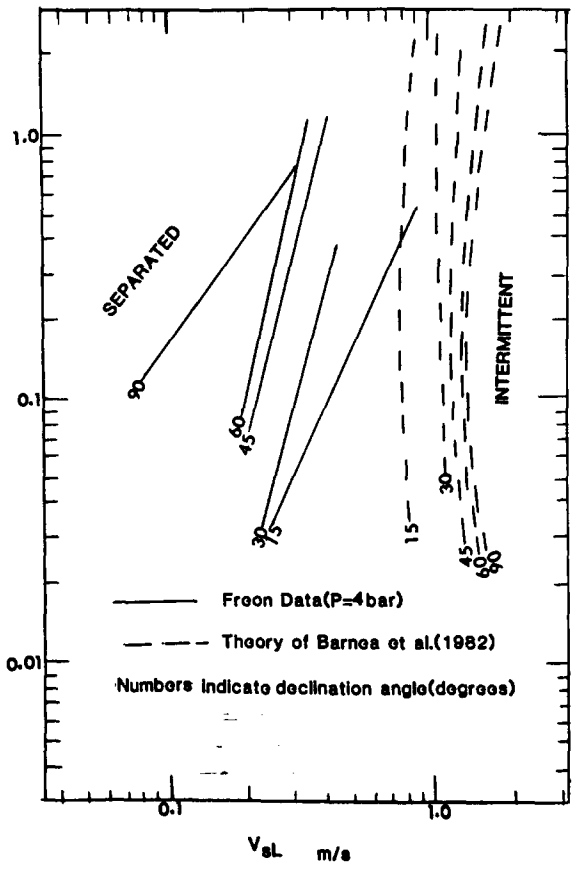

Figure 16. Comparison of freon data and barnea *et al.* predictions of separated–intermittent transition.

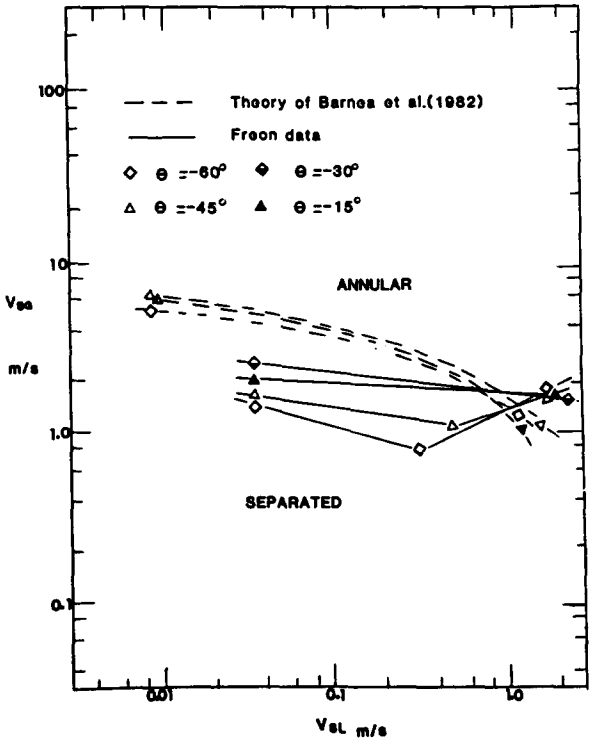

Figure 17. Comparison of freon data and Barnea *et al.* predictions of separated–annual transition.

The prediction of Barnea *et al.* (1982) for the transition from separated (stratified and wavy) to annular flow is compared to the data obtained at ~2 bar in figure 17. It may be seen that fair agreement is obtained. Similar results were obtained for the data at ~4 bar.

Barnea *et al.* (1982) have suggested that at low and moderate void fractions at steep angles, and all angles in slightly declined line, the transition to dispersed bubble flow be obtained from

$$2\left[\frac{0.4\sigma}{(\rho_L - \rho_G)g}\right]^{1/2}\left(\frac{\rho_L}{\sigma}\right)^{3/5}\left[(2/D)C_L\left(\frac{D}{\nu_L}\right)^{-0.2}\right]^{2/5}(V_{SG} + V_{SL})^{(2/5)(3-n)} = 0.725 + 4.15\left(\frac{V_{SG}}{V_{SG} + V_{SL}}\right)^{1/2}, \quad [8]$$

where $C_L = 0.46$ $n = 0.2$

ν_L = kinematic viscosity of liquid = μ_L/ρ_L

m_L = liquid viscosity (M/LT).

This may be rewritten in dimensionless form as

$$2\left[\frac{0.4\sigma}{gD^2(\rho_L - \rho_G)}\right]^{1/2}\left[\frac{D\rho_L(V_{SL} + V_{SG})^2}{\sigma}\right]^{3/5}\left\{2C_L\left[\frac{(\rho_L D(V_{SG} + V_{SL})}{\mu_L}\right]^{-0.2}\right\}^{2/5} = 0.725 + 4.15\left(\frac{V_{SG}}{V_{SG} + V_{SL}}\right)^{1/2} \quad [9]$$

Note that in contrast with the Taitel–Dukler (1976) prediction for horizontal flow, a small surface tension effect is included. This revised expression can be shown to do similar in a number of respects to the dispersed flow transition line of Weisman *et al.* (1979) indicated in figure 3.

The dispersed flow transition data of the present study at ~2 bar are compared with [9] in figure 18. Good agreement is seen. However, at high values of V_{SG}, Barnea *et al.* (1982) predict that for vertically downward lines and lines declined at sharp angles, this transition follows a line of constant void fraction, α. That is,

$$V_{SL} = V_{SG}\left(\frac{1 - \alpha}{\alpha}\right) + (1 - \alpha)V_0 \quad [10]$$

with α set at 0.52 and V_0, the bubble rise velocity, given by

$$V_0 = 1.53\left[\frac{g(\rho_L - \rho_G)_\sigma}{\rho_L^2}\right]^{1/4}$$

The foregoing prediction is shown in the upper portion of figure 18. Although data are limited in that region, there is no indication that the suggested trend is being followed.

7. CONCLUSION

The flow pattern data for downward, co-current, gas–liquid flow has been substantially augmented by the refrigerant 113 tests reported here. These new data allow the effect of gas density to be ascertained. The data from the present study and previous air–water data were compared with recent predictive procedures.

It was found that, for the annular and dispersed flow transitions, the dimensionless correlations used by Weisman *et al.* (1979) and Weisman & Kang (1981) for horizontal and upward flow held also for downward flow. Correlations of the same form as those used by Weisman & Kang (1981) were found to predict the available downflow data on the

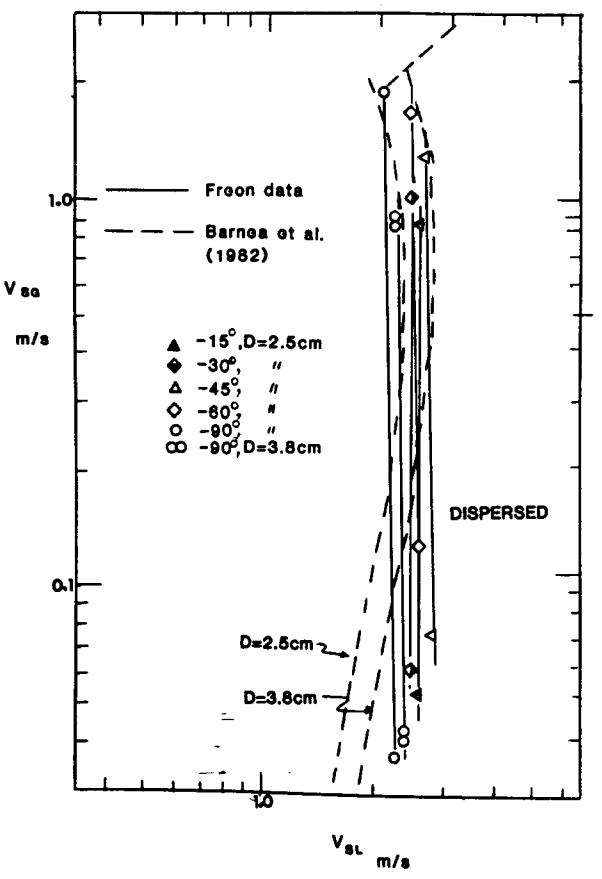

Figure 18. Comparison of freon data to Barnea *et al.* predictions of dispersed flow transition.

bubble–intermittent and separated–intermittent transitions with small modifications. These modifications could be incorporated within the correction factors used for overall flow map devised by Weisman *et al.* (1979) for horizontal flow. It is thus possible to use the same overall flow map for horizontal and downward flow. The map also applies to upward flow in vertical and sharply inclined lines providing it is recognized that the separated flow region no longer exists.

The theoretically based predictions of Barnea *et al.* (1982) have also been compared with the present data. Reasonable agreement between predictions and data were obtained for the transition to dispersed flow at low and moderate void fractions and the transition to annular flow. Only very rough agreement was obtained between the present results and the Barnea *et al.* (1982) predictions for the separated–intermittent transition.

REFERENCES

BARNEA, D., SHOHAM, O. & TAITEL, Y. 1982 Flow pattern transitions for downward inclined two-phase flow, horizontal to vertical. *Chem. Eng. Sci.* **37**, 735–744.

CRAWFORD, T. J. 1983 Analysis of steady-state and transient two-phase flows in downwardly inclined tubes. PhD Dissertation, Drexel University, Philadelphia, PA.

CRAWFORD, T. & WEISMAN, J. 1984 Two-phase (vapor–liquid) flow pattern transitions in ducts of non-circular cross-section and under diabatic conditions. *Int. of Multiphase Flow* **10**, 385–391.

CROWLEY, C. J., SAM, R. G., & WALLIS, G. B. 1984 Slug flow in large diameter pipe: Effect of fluid properties. Paper presented at A.I.Ch.E. Meeting, San Francisco, CA, U.S.A.

GIBSON, J. 1981 Effect of liquid properties, inclination, and pipeline geometry on flow patterns in co-current liquid–gas flow. MS Thesis, University of Cincinnati, Cincinnati, Ohio.

GOLAN, L. P. & STENNING, A. H. (1969) Two-phase vertical flow maps. *Proc. Institution of Mech. Engs.* **184,** 105–114.

IWASYK, J. M. & GREEN, D. A. 1982 Effect of liquid viscosity of annular and intermittent two-phase flow patterns. Paper presented at AIChE Meeting, Los Angeles, CA, U.S.A.

OSHINOWO, T. & CHARLES, M. E. 1974 Vertical two-phase flow. Part IV: Flow pattern correlations. *Can. J. Chem. Eng.* **52,** 25–35.

PEARCE, D. L. 1982 Two-phase flow regimes in horizontal tubes. Paper No. A2/4, European Two-Phase Flow Meeting, Paris.

SPEDDING, P. L. & NGUYEN, V. T. 1980 Regime maps for air–water two-phase flow. *Chem. Eng. Sci.* **35,** 779–793.

TAITEL, Y. & DUKLER, A. E. 1976 A model for predicting flow regime transition in horizontal and near-horizontal flow. *A.I.Ch.E. J.* **22,** 47–55.

WEISMAN, J. 1977 Experimental data on two-phase ΔP across area changes during transients. U.S. Nuclear Regulatory Commission Rep. NUREG-0306.

WEISMAN, J. 1984 Use of simple flow maps for the prediction of the transition to annular and dispersed flow. Paper presented at Int. Symposium on Two-Phase Annular and Dispersed Flows, Pisa, Italy.

WEISMAN, J., DUNCAN, D., GIBSON, J. & CRAWFORD, T. J. 1979 Effects of liquid properties and pipe diameter on two-phase flow patterns in horizontal lines. *Int. J. of Multiphase Flow* **5,** 437–462.

WEISMAN, J. & KANG, S. Y. 1981 Flow pattern transitions in vertical and upwardly inclined lines. *Int. J. of Multiphase Flow* **7,** 271–291.

YAMAZAKI, Y. & YAMAGUCHI, K. 1979 "Characteristics of co-current two-phase downflow in tubes. *J. of Nuc. Sci. & Technol.* **16,** 245–255.